# The Structure of α-Gallium and Its Relationship to Deltahedral Clusters

**Ulrich Häußermann,* Sergei I. Simak, Igor A. Abrikosov and Sven Lidin**

**Abstract**: We present idealised geometrical models for the α-Ga and β-Ga structures based on two differently distorted, corrugated $3^6$ nets. We investigated the structural stability of two sets of two-dimensional and three-dimensional model structures consisting of these corrugated nets as a function of the net puckering. We used the simple tight-binding (TB) Hückel model with the structural energy difference theorem and the advanced full-potential linear muffin-tin orbital (FP-LMTO) method in the framework of local-density functional theory. Both methods show the existence of an optimum puckering angle that corresponds well to the situation in the experimental α-Ga structure. The geometrical model of the α-Ga structure follows the building principle of terminally coordinated deltahedral clusters, extended to two-dimensional structures. The chemical bonding in α-Ga is interpreted in terms of multicentre bonding within the corrugated $3^6$ nets and two-electron–two-centre bonds connecting these nets.

**Keywords**
ab initio calculations · clusters · electronic structure · gallium · semiempirical calculations

## Introduction

Owing to their structural diversity, compounds exhibiting multicentre bonding form one of the most fascinating areas in inorganic chemistry, covering both molecular units and infinite solids.[1, 2] Classical examples are the closed deltahedral clusters formed by B or Ga atoms. These clusters occur as isolated units in boranes or form three-dimensional frameworks in main group metal borides and gallides.[3, 4] Characteristically the cluster-forming atoms are coordinated by an additional atom, which is oriented radially outwards from the polyhedron, leading to a (1 + 3), (1 + 4) or (1 + 5) coordination depending on the kind of polyhedron.

The electronic structure of those clusters is qualitatively expressed by Wade's rules.[5] According to Wade the sp bonding electronic states of a terminally coordinated closed deltahedron with $n$ vertices ($n \geq 5$) are divisible into $n + 1$ framework bonding and $n$ terminally bonding states. In the closed-shell case ($4n + 2$) electrons occupy these bonding states. This corresponds to two-electron–two-centre (2e 2c) bonding of the terminal atoms and multicentre bonding between the atoms forming a polyhedron. Assuming that the terminal atoms are hydrogen, the optimum valence electron concentration (VEC) is $(4 + 2/n)$ electrons per X–H unit. Figure 1 shows the relationship between VEC and the number of vertices $n$ in the series of closed deltahedra. The contribution of $2/n$ to the VEC stems from the lowest-lying electronic state. This nondegenerate state is characteristic of a deltahedral cluster and has highest symmetry with equal contribution from all polyhedron-forming X atoms.

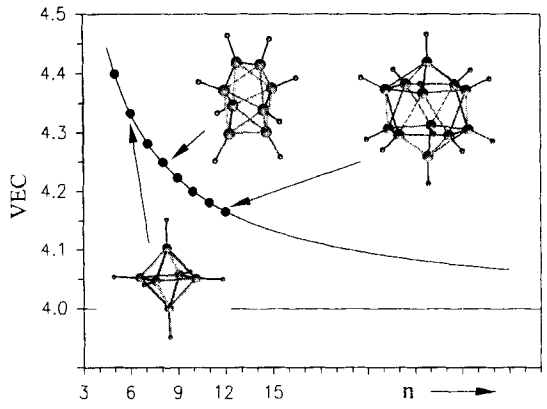


Figure 1. Three examples of terminally (H) coordinated closed deltahedral clusters. In the octahedron (left) all cluster-forming atoms have (1 + 4) coordination, and in the icosahedron (right) (1 + 5) coordination. In the dodecahedron (centre) (1 + 4) and (1 + 5) coordination occurs. The relationship between the optimum VEC (no. of valence electrons per X–H unit) of a cluster and the number of vertices $n$ is given by VEC = $(4 + 2/n)$ as expressed in Wade's rules. Known representatives following this rule are indicated by black circles on this curve.

It is interesting to speculate whether it is possible to realise the asymptotic situation of one terminal-bonding and one framework-bonding state per X–H unit leading to an optimum VEC of four. An infinite value for $n$ is equivalent to a two-dimensional net, and terminal bonding may result in a three-dimensional structure on the borderline between metal and nonmetal. In this

[*] Dr. U. Häußermann, Prof. S. Lidin
Department of Inorganic Chemistry 2, Lund University
P. O. Box 124, 22100 Lund (Sweden)
Fax: Int. code + (46) 222-4012,
e-mail: ulrich@lindstrom.oorg2.lth.se
Dr. S. I. Simak, Dr. I. A. Abrikosov
Department of Condensed Matter Theory, Uppsala University
P. O. Box 530, 75121 Uppsala (Sweden)



0947-6539/97/0306-0904 $ 17.50+.50/0

article we identify the α-Ga structure to be—geometrically and electronically—such a two-dimensional continuation of the terminally coordinated closed deltahedral clusters, in agreement with suggestions of von Schnering and Nesper.[6] We first outline the geometrical building principle of idealised deltahedral clusters and derive two-dimensional (2D) and three-dimensional (3D) model structures obeying this principle. The model structures consist of (1+6)-coordinated atoms. In the second part of this work we study the structural stability of the model structures with the simple semiempirical tight-binding (TB) and the ab-initio full-potential linear muffin-tin orbital (FP-LMTO) methods. The TB method allows additionally the investigation of the influence of the VEC, but does not yield reliable numerical results. However, a modified TB model has been applied succesfully for the geometry optimisation of α-Ga and some other selected structures,[7] and it is interesting to compare results from this method with those obtained from accurate state-of-the-art density-functional calculations.

## Structural Relationships

When building up a closed convex polyhedron with equilateral triangles only (corresponding to a deltahedral cluster with all bond lengths equal), one finds eight possible solutions. The smallest representative in this series is the tetrahedron (**1**) with four vertices, followed by the trigonal bipyramid (**2**), the octahedron (**3**), the pentagonal bipyramid, the dodecahedron (bisdisphenoid) (**4**), the tricapped trigonal prism, the bicapped quadratic antiprism and finally the icosahedron (**5**) with twelve

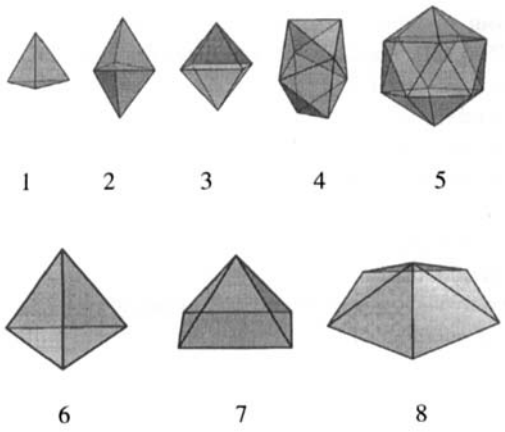


vertices. In these polyhedra a vertex can be shared by either three, four or five triangles, and thus a particular vertex has either three, four or five neighbours. In the following we call an ensemble of three, four or five triangles defining a vertex a tetrahedral cap (**6**), an octahedral cap (**7**) or an icosahedral cap (**8**), respectively. The Platonic polyhedra tetrahedron, octahedron and icosahedron each contain only one kind of vertex; this implies that all angles between connected triangles (the dihedral angles) are equal. With variable dihedral angles polyhedra with two symmetrically different vertices may be built up. For example, the trigonal bipyramid has three three- and two four-coordinated vertices and the dodecahedron (bisdisphenoid) four four- and four five-coordinated vertices.

Naturally the curvature of a polyhedral cap decreases with the number of triangles. It is not possible to construct a convex polyhedral cap with six equilateral triangles, and the condition of equal dihedral angles leads to the planar $3^6$ net. With varying dihedral angles one obtains corrugated 2D nets, and the simplest distortion variants are shown in Figure 2. In variant I adja-

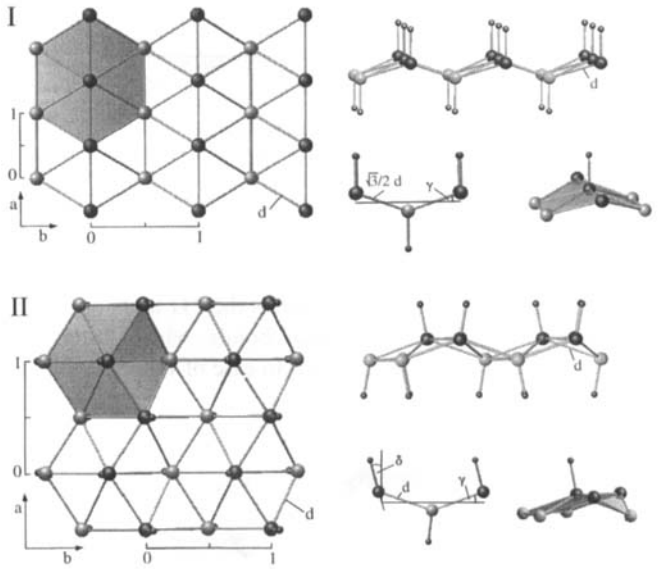


Figure 2. Left-hand panel: Distortion variants of the $3^6$ net consisting of equilateral triangles. Darker circles are the same distance above the undistorted $3^6$ net plane as the brighter circles are below. The net of higher symmetry (top) is called variant I, that of lower symmetry (bottom) variant II. Right-hand panel: Terminal coordination of the net-forming atoms. The corrugated nets are viewed along the $a$ axis. The angle $\gamma$ quantifies the puckering of the $3^6$ nets. The terminal bonds in variant II (bottom) are tilted from the normal of the mean $3^6$ net plane by the angle $\delta$. The different (1+6) coordinations of the net-forming atoms are shown.

cent straight chains and in variant II adjacent zigzag chains of atoms are alternately lowered and raised by the same amount with respect to the undistorted $3^6$ net plane. Variant I has the plane group symmetry *p2mm* with two atoms in the rectangular unit cell, whereas in variant II the mirror planes perpendicular to one axis are lost and the plane group symmetry reduces to *pm* with four atoms per unit cell. The puckering angle $\gamma$ defined in Figure 2 describes the deviation from planarity. The polyhedral caps (**6**–**8**) with all dihedral angles smaller than 180° transform in variant I into an arrangement where six connected triangles form two coplanar sets (in which the dihedral angles are equal to 180°). The corresponding ensemble of variant II exhibits a convex and a concave part on the same surface (Figure 2).

Analogously to in the closed deltahedral clusters in Figure 1, the net-forming atoms may be coordinated terminally. These terminating atoms are arranged in such a way as to minimise interaction with the net-forming atoms. Thus, the sum of distances of a terminating atom to all net-forming ones was chosen to be a maximum for a given bond length. With this condition the terminal bonds of variant II are not perpendicular to the undistorted $3^6$ net plane, and the tilt angle $\delta$, defined in Figure 2, describes this deviation. In Figure 3 the nonlinear relationship between this angle and the puckering angle $\gamma$ is shown. Whereas deltahedral clusters have no structural freedom for a fixed bond

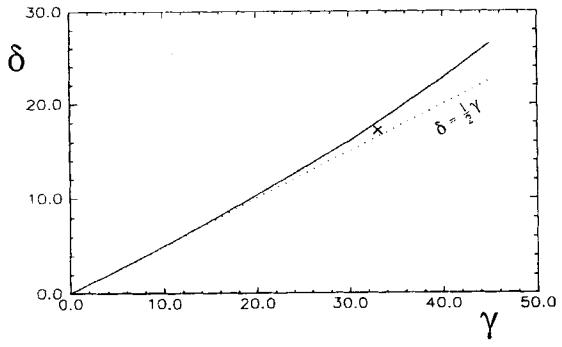


Figure 3. Relation between the puckering angle $\gamma$ and the tilt angle $\delta$ in the terminal coordinated nets of variant II (cf. Figure 2). The cross indicates the values in the experimental α-Ga structure.

length, their 2D analogues shown in Figure 2 show variable puckering angles $\gamma$.

In order to build up 3D structures the 2D units are stacked and linked through the terminal bonds, which leads to orthorhombic structures (Figure 4). In case of variant I the space

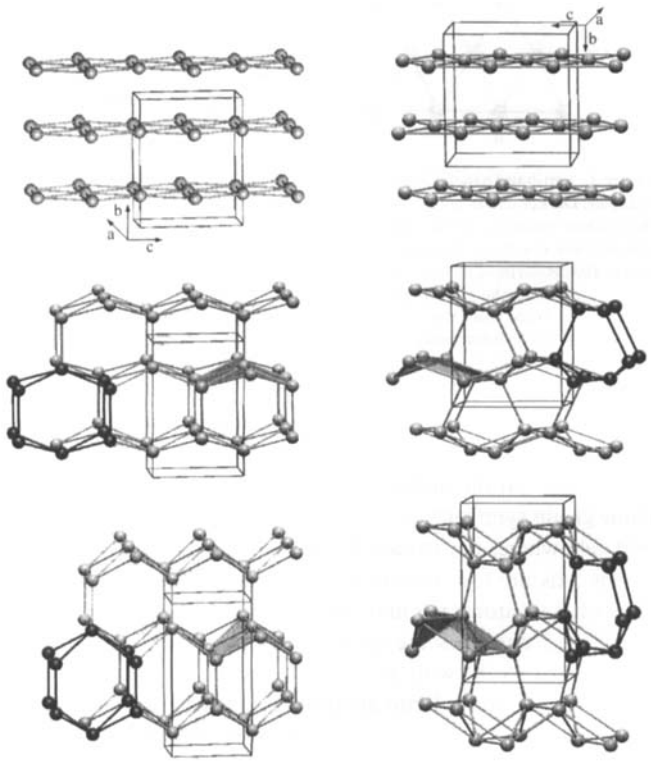

Figure 4. 3D model structures with *Immm* symmetry (left-hand panel) and *Cmca* symmetry (right-hand panel) obtained by stacking of the corrugated nets of variant I and II, respectively, with puckering angles of 0 (top), 25 (centre) and 35° (bottom). Four-, five- and six-membered rings emerge as new structural elements (defining atoms are represented as dark circles). The local (1+6) coordination is emphasised (the *Cmca* structure with $\gamma = 25°$ does not have the appropriate tilt angle).

group is *Immm* with four atoms in position 4g (0,$y$,0). For the 3D structure of variant II the space group in the standard setting is *Cmca* with eight atoms in position 8f (0,$y$,$z$). For a pair of *Immm* and *Cmca* structures with the same geometrical parameters (i.e. puckering angle, distance in the corrugated $3^6$ net, stacking distance), the latter always has the higher density. It is important to note that a stacking of the corrugated $3^6$ nets of variant II with the appropriate tilt angle for the terminal bonds (Figure 3) will automatically fix the stacking distance at a certain value. This causes an unrealistically long bond lenth for the terminal bond in structures with lower values of $\gamma$ (<25°) and an unrealisticly short distance in those with high $\gamma$ values (>35°). For a puckering angle of 32.5° the corresponding tilt angle is 17.6° (Figure 3), and variant II represents an idealised geometrical model of α-Ga, the low-pressure and low-temperature phase of gallium (space group *Cmca*, $a = 4.5192$, $b = 7.6586$, $c = 4.5268$ Å at 298 K; atomic position 8f (0,$y$,$z$) with $y = 0.1549$ and $z = 0.0810$).[8] The structure is shown in Figure 5. In the corrugated $3^6$ net, three slightly different

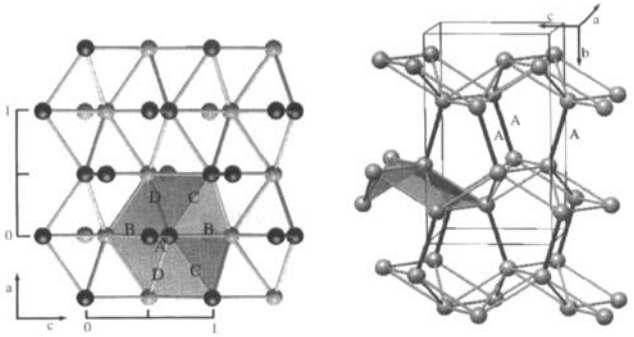


Figure 5. The structure of α-Ga. Left: The 2D building block is a corrugated $3^6$ net parallel to the (010) plane. Darker circles are the same distance above the mean plane of the corrugated $3^6$ net as the brighter circles are below. Three distances occur in the corrugated nets: $B = 2.691$, $C = 2.729$, $D = 2.786$ Å. The coordination by the adjacent nets introduces a short distance $A = 2.484$ Å. Right: View approximately along [100] showing the stacking of the corrugated $3^6$ nets along the $b$ axis through short type $A$ bonds (2.483 Å). The (1+6) coordination of an atom is emphasised.

nearest-neighbour distances lie in the narrow range between 2.69 ($B$) and 2.79 Å ($D$). The distance $A$ between Ga atoms from adjacent nets is 2.483 Å . The angle $\gamma$ in the zigzag chain of $B$ bonds is 32.8°, and the angle between the bond $A$ and the $b$ axis perpendicular to the corrugated $3^6$ net is 17.2°. The agreement with the idealised model is remarkable (cf. Figure 3). Thus, with the short distance $A$ designated as a terminal bond, the α-Ga structure obeys the building principle of ideal deltahedral clusters, where the terminally bonded atoms minimise their interaction with other polyhedron-forming ones by means of their radial orientation. Following this principle, the increase in the coordination number from (1+5) of an icosahedral cap to (1+6) is accompanied by the formation of 2D nets, thus explaining the local coordination of the Ga atoms in the α-Ga structure. This interpretation is different from that of Nesper and von Schnering,[6] who divided the corrugated $3^6$ net into the α-Ga structure in units of distorted (1+5) coordinated icosahedral caps and tetrahedra.

The structure resulting from the stacking of the 2D nets of variant I does not represent a known elemental structure, but occurs as the partial structure of the major component in intermetallic compounds with the $MoPt_2$ structure. In this structure type the voids along the $a$ axis are occupied yielding a binary compound with composition 1:2. Interestingly, the *Immm* structure with a $\gamma$ of 49° can be transformed into an idealised β-Ga structure by a slip operation[9] in every plane (020) with the displacement vector $\vec{R} = (0,0,{}^1/_2)$ (Figure 6). The corrugated $3^6$



0947-6539/97/0306-0906 $ 17.50+.50/0 Chem. Eur. J. 1997, 3, No. 6

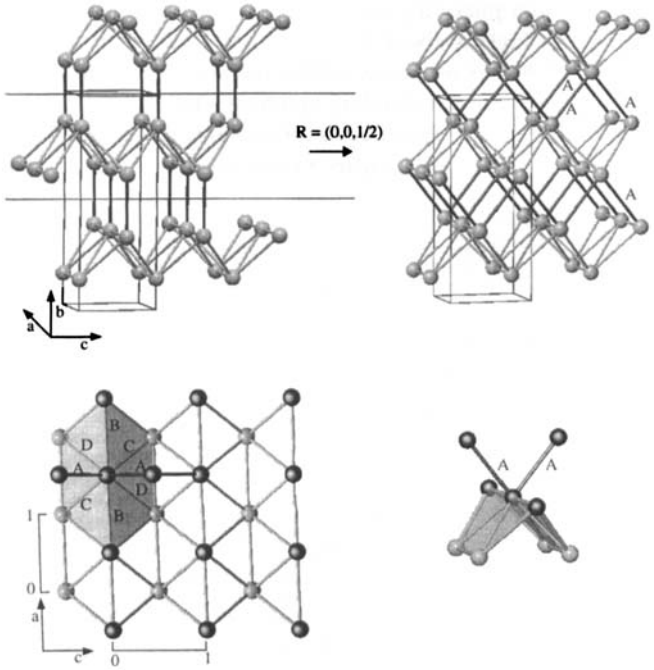


Figure 6. Top: A crystallographic slip operation in the planes (020) with the displacement vector $\vec{R} = (0,0,^1/_2)$ transforms the *Immm* model structure consisting of corrugated $3^6$ net with a puckering angle of 49° (left) to an idealised model of the β-Ga structure. The stacking of the corrugated $3^6$ nets in the monoclinic β-Ga structure (right) introduces zigzag chains defining the shortest distances (labelled *A*) in this structure ($A = 2.689$ Å). Bottom: In the corrugated $3^6$ net of β-Ga (parallel to the (010) plane) three different distances occur: $B = 2.771$, $C = 2.872$, $D = 2.916$ Å. The atoms in β-Ga have a local (2+6) coordination (right).

nets of variant I remain unchanged, but the terminal bonds are replaced by zigzag chains running along the *c* axis. The *Immm* structure may be too open for a metal, so that it collapses according to this slip operation, which changes the nearest-neighbour coordination of the atoms from (1+6) to (2+6). In the real β-Ga structure (space group *C2/c*, $a = 2.7713$, $b = 8.0606$, $c = 3.3314$ Å, $\beta = 91.57°$; atomic position (0,*y*,1/4) with $y = 0.131$)[10] three different distances between 2.77 and 2.92 Å occur in the corrugated $3^6$ net, and the deviation from the model with only equilateral triangles in this net is greater than in the α-Ga structure. The distance in the zigzag chains (2.69 Å) is not much shorter than those in the corrugated $3^6$ net, owing to the increase in the coordination number.

## Calculational Methods

**TB calculations**: Eigenvalues were obtained by solving the Hückel secular determinant $|H_{ij}(\vec{k}) - \varepsilon I| = 0$ with the unit matrix *I* and the atomic parameters of Ga ($H_{4s4s} = -14.58$ eV, $H_{4p4p} = -6.75$ eV, $\zeta_{4s} = 1.77$, $\zeta_{4p} = 1.55$) and H ($H_{1s1s} = -13.6$ eV, $\zeta_{1s} = 1.3$). The resonance integrals were approximated by the Wolfsberg–Helmholtz formula $H_{ij} = {}^1/_2 KS_{ij}(H_{ii} + H_{jj})$ with $K = 1.75$.[11]

In order to compare structural energy differences within the TB formalism we applied the energy difference theorem of Pettifor [Eq. (1)].[12] $E^{\text{bond}}$ has the form given by Equation (2), where $n_i(\varepsilon)$ is the partial density of states

$$\Delta E^{tot} \approx \Delta E^{\text{bond}}|_{\Delta E^{\text{rep}} = 0} \quad (1)$$

$$E^{\text{bond}}(\varepsilon_F) = \sum_i \int_{-\infty}^{\varepsilon_F} (\varepsilon - \varepsilon_i) n_i(\varepsilon) d\varepsilon \quad (2)$$

of the atomic orbital *i*, which we calculated from a Mulliken population analysis.[13] $\varepsilon_i$ is the corresponding orbital energy $H_{ii}$ and $\varepsilon_F$ the Fermi energy.

The sum is over all atomic orbitals of the system. Because of Equation (3)[14] the constraint $\Delta E_{\text{rep}} = 0$ is equivalent to $\Delta\mu_2 = 0$. The quantity $\mu_2$ is

$$\mu_2 = \int_{-\infty}^{+\infty} \varepsilon^2 n(\varepsilon) d\varepsilon = \sum_{i,j} H_{ij}^2 \propto E_{\text{rep}} \quad (3)$$

called the second moment,[15] and the equality of $\mu_2$ between different structures can be achieved by isotropically changing the volumes of the structures until their second moments match that of a reference structure (second moment scaling[16]). Differences in the higher moments $\mu_n = \int_{-\infty}^{+\infty} \varepsilon^n n(\varepsilon) d\varepsilon$ of these structures can explain the behaviour of their structural energy curves.[17]

As reference structure for the $\mu_2$ scaling in the 2D case we chose the corrugated $3^6$ net of the α-Ga structure. This net was coordinated with terminal H atoms at experimentally based distances of 1.6 Å in the direction of the net linking *A* bonds in the α-Ga structure. Nets of variants I and II were constructed with puckering angles of 0, 5, 10, 15, 20, 22.5, 25, 27.5, 30, 32.5, 35, 40 and 45°. The nets were terminated with H atoms in the way described, and the bond length was maintained at a value of 1.6 Å while adjusting the Ga–Ga distance in the net during the second-moment scaling. For the 3D structures the experimental α-Ga structure served as reference structure for the $\mu_2$ scaling. Only the interlayer bond length was varied in the scaling procedure, and the parameters of the final 3D structures are presented in Tables 1 and 2. For the 2D structures a 100 *k*-point mesh and for the 3D structures a 64 *k*-point mesh of the irreducible wedge was used.

Table 1. Parameters of the model structures with *Immm* symmetry.

| Angle (°) | *a* (Å) | *b* (Å) | *c* (Å) | *y* |
|---|---|---|---|---|
| 0 | 2.7305 | 5.8898 | 4.7294 | 0.25 |
| 5 | 2.7243 | 5.9730 | 4.7006 | 0.2328 |
| 10 | 2.7202 | 6.1360 | 4.6399 | 0.2167 |
| 15 | 2.7177 | 6.3704 | 4.5468 | 0.2022 |
| 20 | 2.7166 | 6.6579 | 4.4215 | 0.1896 |
| 22.5 | 2.7166 | 6.8146 | 4.3471 | 0.1839 |
| 25 | 2.7174 | 6.9743 | 4.2657 | 0.1787 |
| 27.5 | 2.7191 | 7.1360 | 4.1774 | 0.1738 |
| 30 | 2.7213 | 7.3014 | 4.0819 | 0.1693 |
| 32.5 | 2.7218 | 7.4869 | 3.9760 | 0.1654 |
| 35 | 2.7292 | 7.6351 | 3.8722 | 0.1612 |
| 40 | 2.7453 | 7.9682 | 3.6425 | 0.1541 |
| 45 | 2.7745 | 8.3085 | 3.3980 | 0.1478 |

Table 2. Parameters of the model structures with *Cmca* symmetry.

| Angle (°) | *a* (Å) | *b* (Å) | *c* (Å) | *y* | *z* |
|---|---|---|---|---|---|
| 0 | 4.7294 | 5.8705 | 5.4610 | 0.25 | 0.125 |
| 5 | 4.7111 | 5.9517 | 5.4261 | 0.2301 | 0.1240 |
| 10 | 4.6837 | 6.1054 | 5.3539 | 0.2113 | 0.1211 |
| 15 | 4.6472 | 6.3294 | 5.2465 | 0.1945 | 0.1172 |
| 20 | 4.5979 | 6.6339 | 5.1030 | 0.1800 | 0.1084 |
| 22.5 | 4.5678 | 6.8160 | 5.0186 | 0.1738 | 0.1036 |
| 25 | 4.5338 | 7.0173 | 4.9266 | 0.1682 | 0.0978 |
| 27.5 | 4.4963 | 7.2332 | 4.8285 | 0.1631 | 0.0911 |
| 30 | 4.4540 | 7.4664 | 4.7242 | 0.1587 | 0.0833 |
| 32.5 | 4.4085 | 7.7066 | 4.6169 | 0.1546 | 0.0743 |
| 35 | 4.3590 | 7.9532 | 4.5079 | 0.1508 | 0.0637 |
| 40 | 4.2502 | 8.4442 | 4.2975 | 0.1432 | 0.0370 |
| 45 | 4.1286 | 8.9013 | 4.1286 | 0.1340 | 0 |

**FP-LMTO Calculations**: Reliable energy differences between the 3D structures (Table 1 and 2) and the experimental α-Ga structure were calculated with the FP-LMTO method,[18] which is a powerful all-electron technique for the calculation of different properties of crystalline materials. The space was divided into so-called muffin-tin spheres (MTS) surrounding atomic sites and interstitial region between them. The charge density and potential were allowed to have any shape inside MTS as well as in the interstitial region. The basis set, charge density and potential were expanded in spherical harmonic series within nonoverlapping MTS and in Fourier series in the interstitial region. The basis set of augmented linear muffin-tin orbitals[19] was used. The

tails of the basis functions outside their parent spheres were linear combinations of Hankel functions with negative kinetic energy. The basis set included 3d, 4s, 4p and 4d orbitals on the Ga sites. All states were contained in the same energy panel with the 3d orbitals treated as a pseudovalence state in an energy set different from the other basis functions. We adopted a double basis where we used two different orbitals of $l,m_l$ character, each connected in a continious and differentiable way to Hankel functions with different kinetic energy. The spherical harmonic expansion of the charge density, potential, and basis functions were carried out to $l = 4$. The integration over the Brillouin zone was performed by the special point sampling[20] with a Gaussian smearing of 10 mRy and using 282 and 171 $k$-points in the irreducible wedge for the *Cmca* and *Immm* model structures, respectively. The exchange and correlation potential was treated in the local density approximation using the von Barth–Hedin parametrisation.[21]

## Results and Discussion

**2D structures**: Figure 7 shows the calculated TB bond energies for the two terminally coordinated distortion variants of the $3^6$ net as a function of the puckering angle and the VEC in a contour-map representation. Qualitatively the maps look alike. The optimum VEC for the uncorrugated nets is slightly above four electrons per Ga–H unit and decreases to exactly four at the optimum puckering angles with lowest bond energy. This puckering angle is about 25° for variant I and 22.5° for variant II. At higher puckering angles the bond energy increases again while the corresponding optimum VEC shifts rapidly to lower values (<4). This effect is considerably more pronounced in the case of variant II. Figure 8 summarises the bond energies

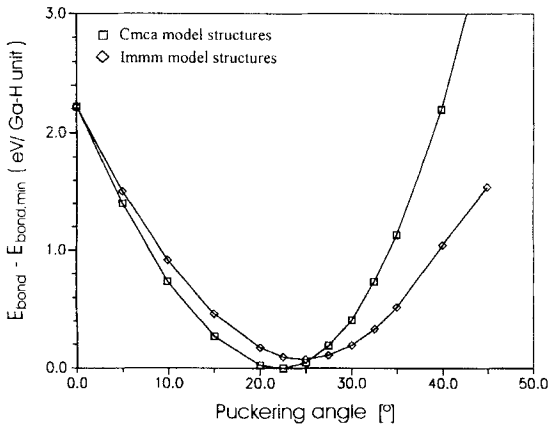


Figure 8. TB bond energy for the 2D nets of variants I and II at optimum values of VEC as a funtion of $\gamma$.

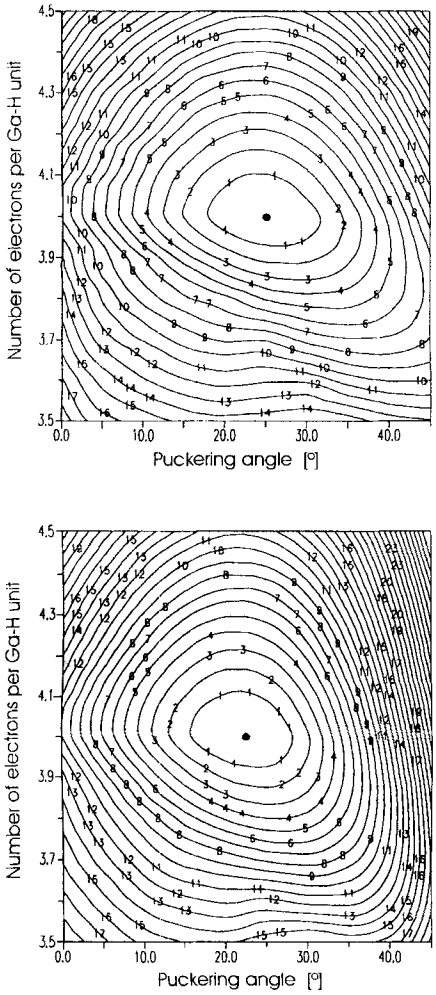


Figure 7. TB bond energy as a function of VEC and $\gamma$ for the 2D nets of variant I (top) and variant II (bottom) (cf. Figure 2). The location of the minima are indicated by solid circles. Contour lines are calculated relative to the minima; the difference between two lines is 0.2 eV.

at the optimum VEC as a function of the puckering angle. Until the optimum puckering angle is reached the curves of variant I and II are very similar and the minimum value for $E^{bond}$ is not significantly different. Within the TB approach the two distortion variants appear as energetically equivalent solutions, and the optimum VEC of four is indeed the expected asymptotic value in the context of Wade's rules (Figure 1).

The shift of the optimum VEC towards lower values can qualitatively be explained with the method of moments.[17, 22] Differences in TB bond energies of two structures are controlled by differences in the higher moments $\mu_n$ ($n > 2$). Such differences originate in simple structural features. Of most influence are changes in $\mu_3$, and this particular moment is determined by the number and form of three-membered rings in a structure. A large number of triangles has the effect of producing a large $|\mu_3|$, and usually the larger $|\mu_3|$ of a structure, the lower is the optimum VEC for maximum structural stability. For low values of $\gamma$ the puckering procedure does not influence the number or form of the triangles, and so $|\mu_3|$ is almost constant. With increasing puckering angle, additional interactions between net-forming atoms situated in neighbouring chains at the same height are possible, which enlarges the number of triangles. The accompanying increase in $|\mu_3|$ changes the optimum VEC to lower values.

**3D structures**: Figure 9 shows the contour maps of the TB bond energies for the two sets of 3D structures. For both sets the optimum VEC for the unpuckered structure is about 2.5 electrons per atom and increases to a value slightly below the expected three at an optimum puckering angle of 30°. The change of the value of the optimum $\gamma$ compared to the 2D case is due to the change in the environment of the corrugated $3^6$ nets in the 3D structures. The stacking of the nets creates new structural elements (Figure 4), which certainly influence the optimum



0947-6539/97/0306-0908 $ 17.50+.50/0 Chem. Eur. J. 1997, 3, No. 6

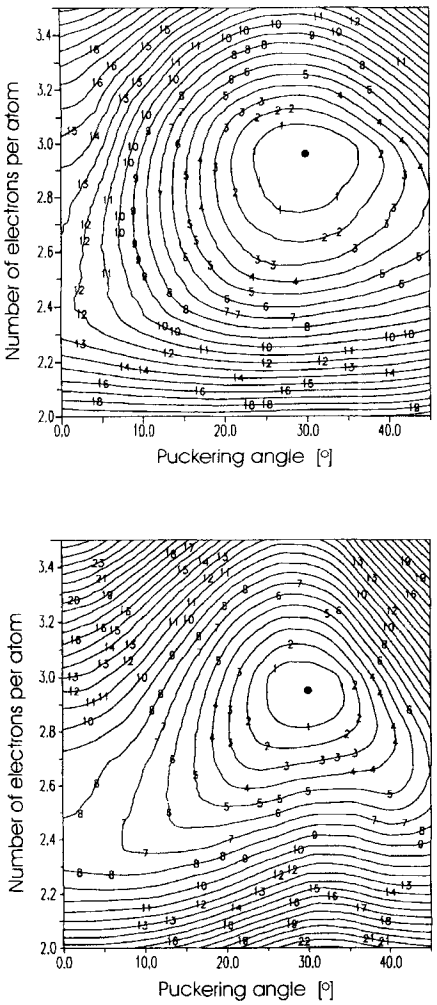


Figure 9. TB bond energy as a function of VEC and $\gamma$ for the 3D structures with *Immm* symmetry (top) and *Cmca* symmetry (bottom) (cf. Figure 4). The location of the minima are indicated by solid circles. Contour lines are calculated relative to the minima; the difference between two lines is 0.2 eV.

puckering angle of the corrugated $3^6$ nets from an electronic point of view. Besides, by assuming that the α-Ga structure follows the building principle of deltahedral clusters (e.g. shorter distances to terminal atoms which have bonding interaction with only one net-forming atom), a 3D structure can only be built up when $\gamma \geq 30°$. Hoistad et al. performed a geometry optimisation of the experimental α-Ga structure with the same TB model; they were able to reproduce the experimental value of the puckering angle, but obtained a tilt angle that was slightly too large.[7]

Again, changes in $|\mu_3|$ qualitatively accounts for the behaviour of the optimum VEC as a function of $\gamma$. The unpuckered structure has a large $|\mu_3|$ as it contains interlayer as well as intralayer triangles. During the puckering procedure the influence of the latter reduces gradually, and so $|\mu_3|$ of the puckered structures decreases until, analogously to the 2D case, additional interlayer triangles arise. The lowering of $|\mu_3|$ stabilises the puckered structures at a VEC of around three relative to the unpuckered structure, and the values of the optimum VEC follow these changes of $|\mu_3|$, as the structure with the higher $|\mu_3|$ has its stability maximum at lower VEC. Along the structural route described by the puckering procedure, the model structure of α-Ga is the solution with minimum $|\mu_3|$ and, on the basis of this fact, Lee et al. developed an alternative interpretation of the α-Ga structure.[16] In contrast to our focus on the local (1+6) coordination of the atoms in this structure, they emphasise the relationship between the number of triangles of interacting atoms and the VEC. Hence, the α-Ga structure is the result of optimising the number of triangles for a VEC of three. Compared to the simple packing structure types fcc, hcp and bcc, which are stable at lower VEC, the number of triangles has to be reduced when considering sp-bonded systems.

In the TB approach the higher symmetry *Immm* structures appear to be more stable than the corresponding *Cmca* structures when $\gamma > 15°$. In Figure 10 the TB and FP-LMTO results

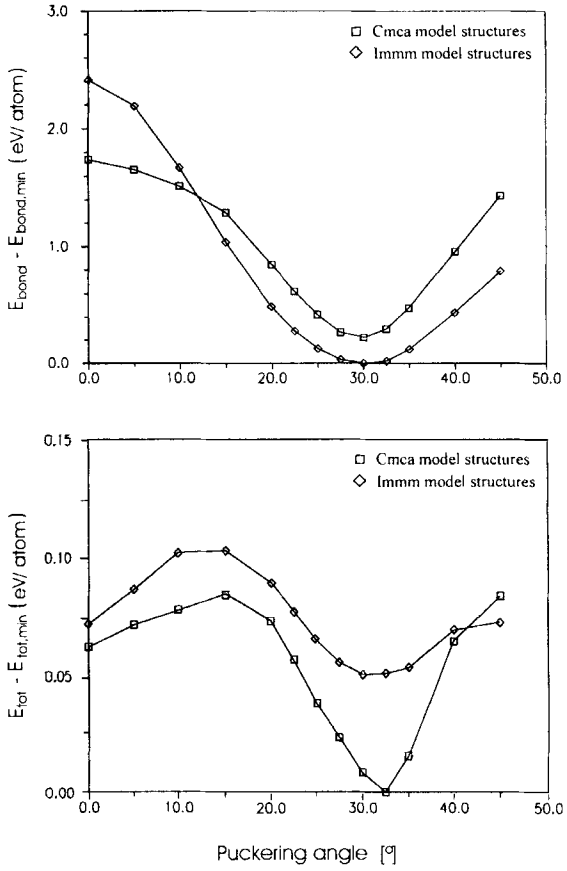


Figure 10. TB bond energies at optimum values of VEC (top) and FP-LMTO total energies (bottom) for the 3D model Ga structures with *Immm* and *Cmca* symmetry as a funtion of $\gamma$.

are shown for comparison. For the structures with $\gamma > 15°$ the energy versus $\gamma$ curves look similar to the TB curves and show an optimum $\gamma$ value of about 30° for the *Immm* structures and about 32.5° for the *Cmca* structures. However, the *Cmca* structures lie lower in energy and the minimum at $\gamma \approx 32.5°$ corresponds more closely to the situation in the experimental α-Ga structure. The TB bond energies obtained with the second moment scaling procedure[7, 12, 16] gave reliable results for the optimisation of bond angles, but failed in the prediction of the correct ground state for structures with different symmetry. The numerical results from a TB model can certainly be influenced

by the choice of the atomic parameters and the approximation of the repulsive energy.[14]

In Figure 11 we show the total energy as a function of the atomic volume for the experimental α-Ga structure and for the *Cmca* and *Immm* Ga model structures with their optimum puckering angles of 32.5 and 30°, respectively. The distortion from

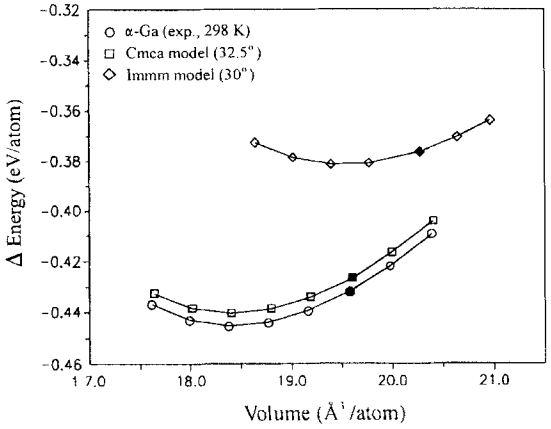


Figure 11. Total energy differences of the *Cmca* and *Immm* model structures with optimum puckering angle and of the α-Ga structure as a function of volume calculated with the FP-LMTO method. Solid symbols indicate the unrelaxed structures.

the idealised *Cmca* model structure with only one set of nearest-neighbour distances in the corrugated $3^6$ net stabilises the experimental α-Ga structure by only about 0.005 eV per atom. The calculated equilibrium volume of the *Immm* model structure is about 5% higher than that of the experimental α-Ga structure. The energy difference between these two structures is about 0.06 eV per atom.

It is instructive to study the changes in the ratio between the total number of p and s states calculated inside the Ga MTS for the two sets of model structures (Figure 12). Comparing the bonding situation in structures of isoelectronic elements with four or fewer valence electrons, a high total number of p states is characteristic for directional, covalent bonding, whereas a high total number of s states indicates a more metallic character of chemical bonding. Thus the ratio between these two numbers

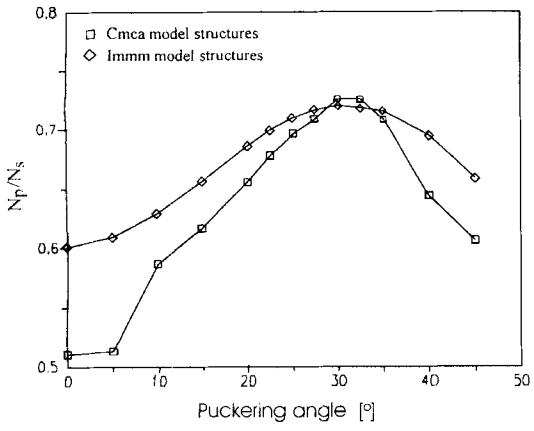


Figure 12. Ratio between the total number of p states ($N_p$) and s states ($N_s$) inside the Ga MTS obtained from FP-LMTO calculations for the *Immm* and the *Cmca* model structures.

can be used as a measure of the relative decrease or increase of covalency in the complex bonding situation of structures on the metal/nonmetal borderline. Figure 12 demonstrates the presence of "maximum covalency" for the *Cmca* and *Immm* model structures when the puckering angle is in the range of 30–32.5°. This fact indicates the importance of covalency, that is, terminal 2e2c bonding, in the formation of the most stable model structures under consideration.

## Concluding Remarks

We demonstrated that the α-Ga structure follows the building principle of deltahedral clusters, which gives terminally coordinated corrugated $3^6$ nets as 2D building units. Based on this principle it is possible to construct other (hypothetical) structures with (1 + 6)-coordinated atoms at the metal/nonmetal borderline. The presented simplest case, a model structure with higher symmetry than the α-Ga structure, was found to be considerably less stable than α-Ga. Interestingly it is possible to transform this higher-symmetry model structure into the β-Ga structure by a crystallographic slip operation. Recent scanning tunnelling microscopy (STM) investigations on the α-Ga(010) surface[23] and band structure calculations on the α-Ga structure[24, 25] emphasise the shortest bond length between Ga atoms as the main structural feature in this system. Thus, α-Ga is described as a metallic molecular crystal consisting of discrete $Ga_2$ dimers. In contrast, when classifying the short bond length as a terminal 2e2c bond, in analogy to deltahedral clusters, the α-Ga structure appears as a 2D metal. The optimum VEC is three electrons per atom. Boron, in the α-rhombohedral boron structure, realises an alternative, semiconducting solution to this VEC based on $B_{12}$ icosahedra with (1 + 5)-coordinated B atoms. Gallium is a higher homologue to boron and will therefore prefer higher coordination numbers in molecular and extended structures. The structure of α-Ga still follows the building principle of deltahedral clusters, but the increase in the local coordination of the atoms from (1 + 5) to (1 + 6) leads to a metallic structure.

**Acknowledgment**: This work was supported by the Swedish National Science Research Council (NFR) and the Crawfoord foundation. U. H. acknowledges a Feodor-Lynen Fellowship of the A. v. Humboldt Foundation. The FP-LMTO program code was written by J. Wills (Los Alamos). The graphics program for the 3D representation of crystal structures was developed by P. Hofmann.[26] S. I. S. and I. A. A. are grateful to O. Eriksson for valuable discussions.

Received: October 9, 1996 [F488]
Revised version: January 23, 1997

[1] N. N. Greenwood, A. Earnshaw, *Chemistry of the Elements*, Pergamon Press, Oxford, **1989**.
[2] R. Nesper, *Angew. Chem. Int. Ed. Engl.* **1991**, *30*, 789.
[3] a) G. Mair, *Thesis*; University of Stuttgart, Germany, **1984**. b) C. Belin, M. Tillard-Charbonell, *Prog. Solid State Chem.* **1993**, *22*, 59.
[4] Even terminally coordinated closed deltahedral clusters formed by Al atoms have recently been reported: e.g., W. Uhl, *Angew. Chem. Int. Ed. Engl.* **1993**, *32*, 1386.
[5] K. Wade, *Adv. Inorg. Chem. Radiochem.* **1976**, *18*, 1.
[6] H. G. von Schnering, R. Nesper, *Acta Chem. Scand.* **1991**, *45*, 870.
[7] L. M. Hoistad, S. Lee, J. Pasternak, *J. Am. Chem. Soc.* **1992**, *114*, 4790.
[8] J. Donohue, *The Structure of the Elements*, Wiley, New York, **1974**.
[9] B. G. Hyde, S. Andersson, *Inorganic Crystal Structures*, Wiley, New York, **1989**.

[10] a) L. Bosio, A. Defrain, *Acta Crystallogr. B* **1969**, *25*, 995. b) A. Defrain, *J. Chim. Phys. Phys. Chim. Biol.* **1977**, *74*, 851.
[11] M. H. Wangbo, M. Evain, T. Hughbanks, M. Kertesz, S. Wijeyesekera, C. Wilker, C. Zheng, R. Hoffmann, *Program EHMACC: Extended Hückel Molecular and Crystal Calculations; Program EHPC: Extended Hückel Property Calculations*, QCPE Version, 1987.
[12] D. G. Pettifor, *J. Phys. C: Solid State Phys.* **1986**, *19*, 285.
[13] R. S. Mulliken, *J. Chem. Phys.* **1955**, *23*, 1833.
[14] The relation $\sum_{i,j} H_{ij}^2 \propto E_{rep}$ holds for most sp-bonded systems. However deviations might occur, requiring an adjustment of the exponent. See, e.g., M. Shah, D. G. Pettifor, *J. Alloys Compd.* **1993**, *197*, 145.
[15] F. Ducastelle, F. Cyrot-Lackmann, *J. Phys. Chem. Solids* **1971**, *32*, 285.
[16] a) S. Lee, R. Rousseau, C. Wells, *Phys. Rev. B* **1992**, *46*, 12121. b) S. Lee, *Acc. Chem. Res.* **1991**, *24*, 249. c) S. Lee, *J. Am. Chem. Soc.* **1991**, *113*, 101.
[17] a) J. K. Burdett, S. Lee, *J. Am. Chem. Soc.* **1985**, *107*, 3050. b) *ibid.* **1985**, *107*, 3063.
[18] a) J. M. Wills, (unpublished). b) J. M. Wills, B. R. Cooper, *Phys. Rev. B* **1987**, *36*, 3809. c) D. L. Price, B. R. Cooper, *ibid.* **1989**, *39*, 4945.
[19] a) O. K. Andersen, *Phys. Rev. B* **1975**, *12*, 3060. b) H. L. Skriver, *The LMTO Method*, Springer, Berlin, **1984**.
[20] a) D. J. Chadi, M. L. Cohen, *Phys. Rev. B* **1973**, *8*, 5747. b) S. Froyen, *Phys. Rev. B* **1989**, *39*, 3168.
[21] U. von Barth, L. Hedin, *J. Phys. C* **1972**, *5*, 1629;
[22] J. C. Cressoni, D. G. Pettifor, *J. Phys. Condens. Matter* **1991**, *3*, 495.
[23] O. Züger, U. Dürig, *Phys. Rev. B* **1992**, *46*, 7319.
[24] X. G. Gong, G. L. Chiarotti, M. Parrinello, E. Tosatti, *Phys. Rev. B* **1991**, *43*, 14227.
[25] M. Bernasconi, G. L. Chiarotti, E. Tosatti, *Phys. Rev. B* **1995**, *52*, 9988.
[26] P. Hofmann, R. Nesper, *COLTURE: program for the interactive visualisation of crystal structures*; ETH Zürich, 1995.